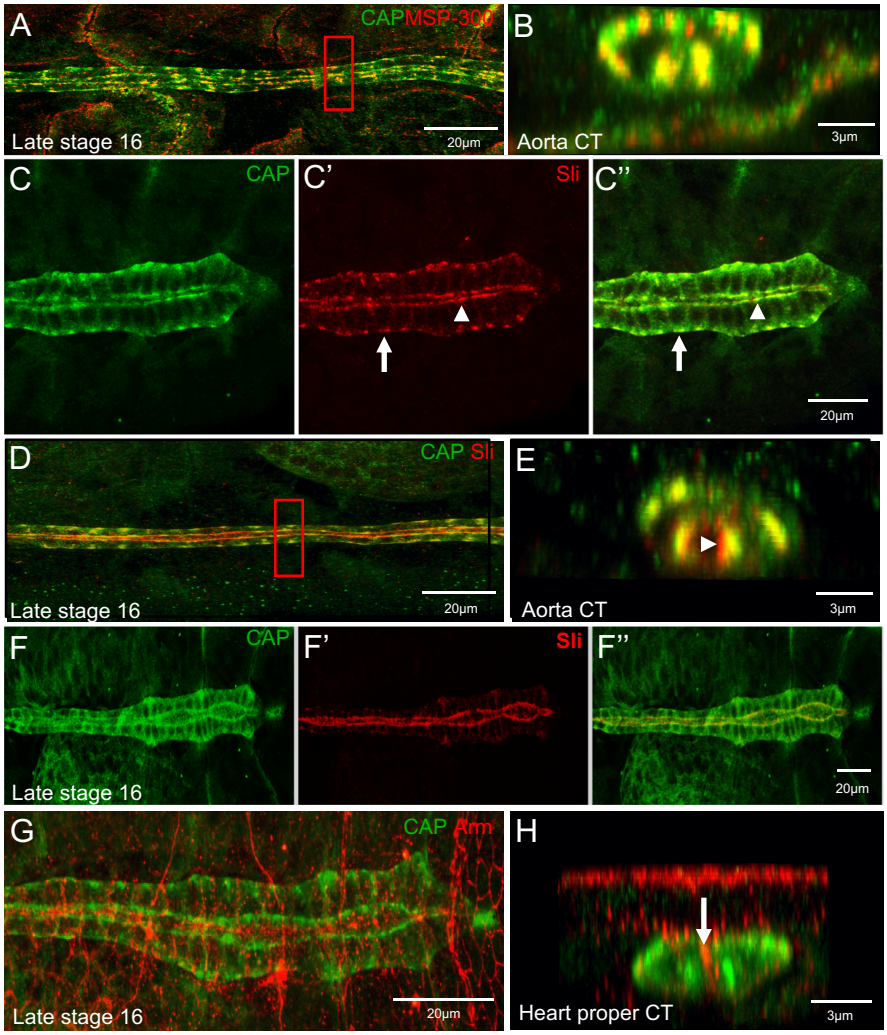

Fig. S1. CAP expression pattern in cardiac cells
(A, B) Dorsal view of a stage 16 embryo showing CAP and MSP300 localization in aorta and 3D reconstruction of transversal cut in aorta (B) validating accumulation of MSP300 and CAP on basal and apical side of CBs.
(C-C") Dorsal view of a stage 16 embryo showing that Slit colocalizes with CAP protein in a similar dotty pattern on apical (arrowheads) and basal sides of CBs (arrows).
(D, E) Dorsal view of a stage 16 embryo showing CAP and Slit localization in aorta and 3D reconstruction of transversal cut in aorta (E) validating accumulation of Slit and CAP on basal and apical side of CBs (arrowhead). Note that Slit protein is secreted at luminal side explaining the partial overlap with CAP.
(F-F") At late stage 16, Slit protein becomes accumulated at the lumen and strongly reduced at the basal side, while CAP is still maintained on both sides.
(G, H) CAP is not colocalized with Armadillo at the adherens junctions between contralateral CBs (arrow).

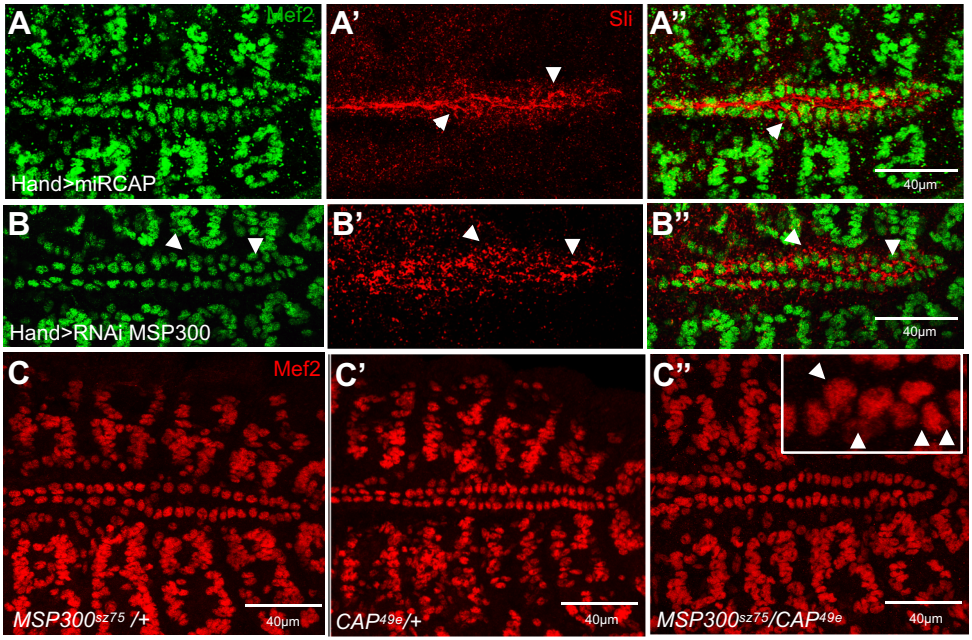

Fig. S2. CAP and MSP300 interact genetically to control CBs alignment and number (A-A") Cardiac specific miR KD of *CAP* using Hand-Gal4 driver induces CBs misalignment and polarity defects visualized with anti-Mef2 and anti-Slit antibodies (arrowheads) similarly to CAP and *MSP300* homozygous mutant. (B-B") Cardiac specific short hairpin KD (TRIP line) of MSP300 using Hand-Gal4 driver induces CBs misalignment and polarity defects visualized with anti-Mef2 and anti-Slit antibodies (arrowheads) similarly to *MSP300* homozygous mutant. (C-C") Immunostaining with anti-Mef2 in *CAP* and *MSP300* single heterozygous (C-C') by comparison with double heterozygous contexts (C"). No apparent change in CBs alignment can be observed in single heterozygous background while clusters of CBs in heart proper are visible in transheterozygous context (C", arrowheads in higher magnification window) demonstrating a genetic interaction between *CAP* and *MSP300* during CBs migration.

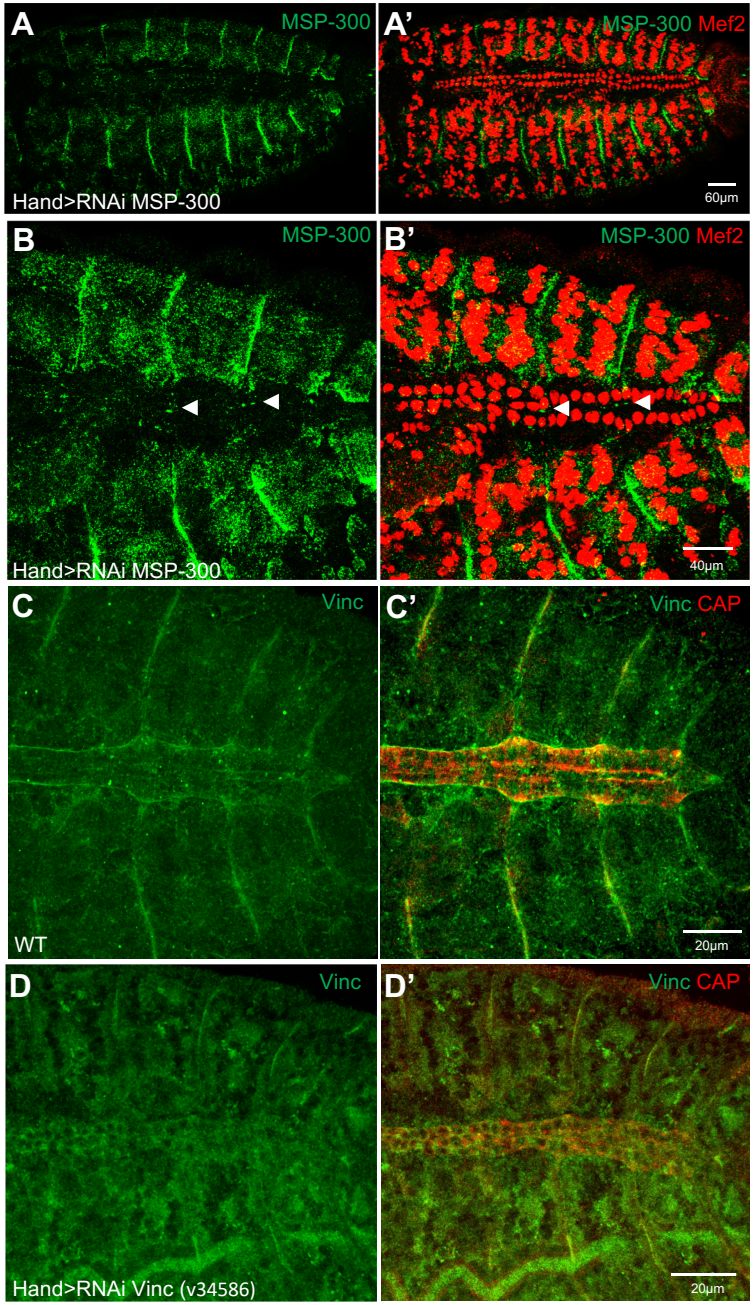

Fig. S3. Validation of RNAi lines targeting MSP300 and Vinc.
(A-B') Dorsal view of stage 16 embryo stained with anti-Mef2 and anti-MSP300 antibodies showing almost complete absence of MSP300 cardiac spots while in somatic muscles MSP300 is still highly present. Arrowheads in higher magnification pictures (B-B') point to remaining MSP300 accumulation.
(C-C') Dorsal view of stage 16 embryo stained with anti-CAP and anti-Vinc antibodies showing almost complete absence of Vinculin in RNAi context (D-D') compared to WT(C-C'). In both cases the HandGAL4 driver was used.

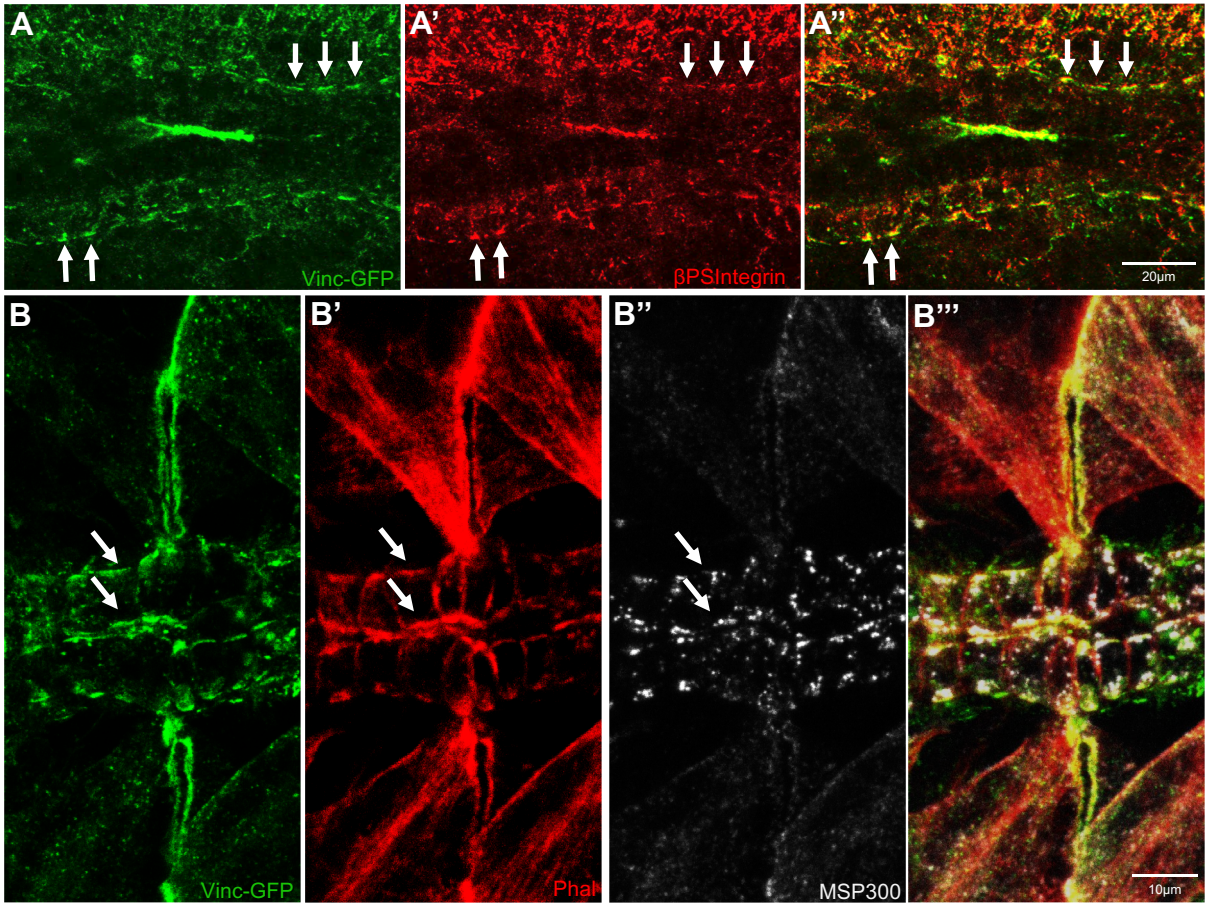

Fig. S4. Vinculin GFP colocalizes with βPS Integrin, F-actin and MSP-300
(A-A") Vinc-GFP colocalizes with bPS Integrin in cardioblasts (arrows) suggesting its involvement in Integrin focal adhesion complex. (B-B"') Dorsal view of stage 16 embryo showing Vinc-GFP colocalization with F-actin and MSP300 on apical and basal sides (arrows) suggesting a focal adhesion-based process connected to the nucleus through F-Actin.

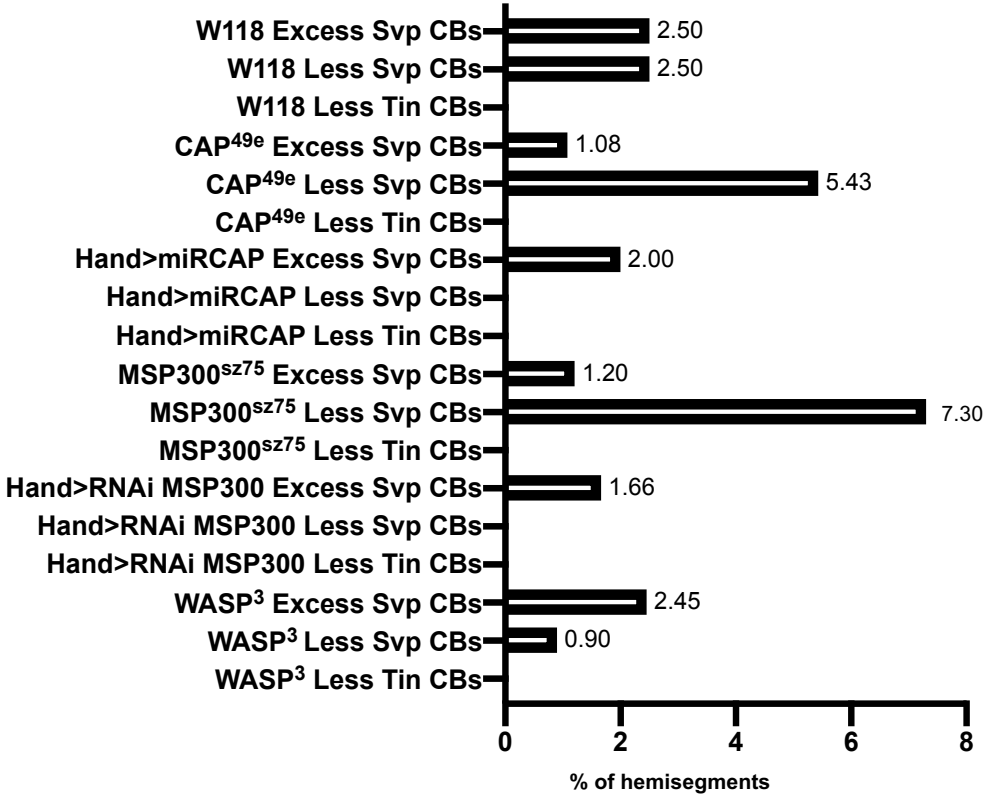

Fig. S5. Bar chart showing the percentage of hemi-segments with changes in CBs number other than an excess of Tin CBs

Data are represented as percentage of hemi-segment presenting either excess Svp +CBs, Less Svp+CBs or less Tin+CBs. (W118 n=240, *CAP49e* n=360, Hand>miRCAP n=240, *MSP300sz75* n=360, Hand>RNAi MSP300 n=240, *MSP300sz75/+* n= 240, *MSP300sz75/CAP49e* n=240, *WASp*^{3} n=240)